GAIT ANALYSIS USING 3D MOTION RECONSTRUCTION WITH AN ACTIVITY-SPECIFIC TRACKING PROTOCOL

Yan Wang, Chieh Chien, James Xu, Gregory Pottie and William Kaiser

University of California, Los Angeles, California 90095
Department of Electrical Engineering

ABSTRACT

In this paper, we present a new gait analysis method using 3D body motion reconstruction with an activity-specific tracking protocol. A kinematic chain modeling the movement of lower extremities was constructed for general lower body activity monitoring. By exploring the nature of walking, a constrained forward-backward statistical linearized sigma-point Kalman Smoother with periodic state vector resetting was developed. This tracks the dynamic joint configuration during walking. Direct experimental evaluation was provided by step length computation as well as complete motion reconstruction. This method has demonstrated stable long term tracking of walking and yields greater than 95% accuracy for step length estimation.

Index Terms— 3D body motion tracking, motion reconstruction, step length estimation.

1. INTRODUCTION

Many of the most urgent problems in health and wellness promotion, diagnostics and treatment of neurological disease require accurate, reliable and detailed monitoring of human motion. For example in the United States alone, approximately 795,000 strokes occur each year. Here the capability to provide remote, in-community monitoring and analysis of lower extremity mobility and its corresponding characteristics is essential for improving exercise tolerance and providing at-home physical rehabilitation, both central in reducing recurrent stroke and myocardial infarction, dependence on others and the cost of care [1, 2]. Now, an urgent need exists for methods that harness low cost wireless inertial sensing platforms to provide accurate and reliable classification of detailed human motion characteristics.

Due to the important benefits demonstrated by the monitoring and analysis of gait characteristics, a number of methods have been proposed that replace the century-old traditional method of manual evaluation. In clinic environments, complex motion laboratory facilities are sometimes used that can obtain accurate tracking of lower limbs with kinematic and force characteristics, however these system are prohibitively expensive outside of major hospitals and they cannot be deployed in the community due to space requirements. In [3], a gait analysis system was developed for detecting strides for patients afflicted with Alzheimers patients. In [4], a template based system is used to determine individual strides of a subject with wearable accelerometers. While there are many more examples of gait analysis methods using inertial sensor data, they all suffer from a major shortcoming: the features obtained are not informative of physical motion characteristics most needed by clinicians. This produces challenges for clinicians who require results critical to evaluation of physical motion for diagnostics or assessment of rehabilitation.

This paper presents a new gait analysis method that exploits an activity-specific tracking protocol to reconstruct 3D motion of lower extremities during walking. The paper provides the following contributions: 1) An activity-specific tracking protocol providing motion characterization without reliance on prior system training; 2) A general trunk-thigh-leg kinematic chain applicable to lower extremity activity modeling; 3) A stable tracking algorithm for long term walking monitoring and gait analysis in 3D space; 4) A linear model to estimate step length with high accuracy as required by clinicians for gait quality assessment.

2. ACTIVITY-SPECIFIC TRACKING PROTOCOL

When analyzing human movements, the human body can be decomposed into 9 segments [5]. To characterize full-body motions, we need to describe joint configuration, rotation angle between each part of body segments [5]. However, to analyze a specific activity, not every joint angle may be of interest. For example, when post-stroke patients are administered with the Wolf Motor Function Test [6], the examiner will focus exclusively on the movements of upper extremity segments and the dynamic configuration of the connecting joints. The development reported here is focused on a new activity-specific tracking protocol where for each activity, only those segments of interest are tracked and the type of the connecting joints as well as their degree of freedom (DOF) will depend on the nature of the activity. In this paper, we focus on the activity-specific tracking protocol applied to walking. This is selected since it provides the most comprehensive test of this new method due to the complex nature of walking. Success in walking characterization then demonstrates applicability of this method to many other activities.

2.1. Kinematic Chain to Characterize Walking

Following the approach applied in robotics, a manipulator is characterized by a kinematic chain, which is equivalent to a sequence of links connected by joints. A 4×4 transformation matrix with 4 parameters, a, α, d and θ can be easily calculated to relate two consecutive links connected by a 1DOF joint after carefully assigning the frame to each link [7]. This convention has been applied to characterize body joint movements by decomposing a multi-DOF joint into a set of 1DOF joints with 0-length links between them [8, 9].

To characterize human walking, segments of interest are the thigh and leg. A kinematic chain may be constructed after performing joint decomposition for the hip and knee joint [8, 9], however, a closer observation reveals that in addition to the segment rotation, a linear translation of the trunk is required to render a comprehensive motion analysis. Thus, three 1DOF pseudo joints are used in the center of the body weight to incorporate the freedom of linear translation.

A joint only allowing rotation about a single axis is a revolute joint while a joint only permitting linear translation along a single axis is prismatic joint. Overall, a 9-1DOF-joint kinematic chain consisting of 3 prismatic joints to characterize body translation and 6 revolute joints to characterize segment rotation can be used to track walking, assuming all the joints of interest have 3 degrees of freedom (Fig. 1).

Since the frame assignment in Fig. 1 strictly follows the D-H convention [7], a 4-parameter transformation matrix T_i^{i-1} can be used to define the frame attached to Link i referenced in the frame of its adjacent Link $i-1$

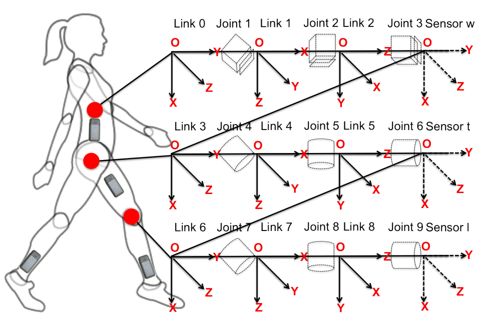

Fig. 1: Kinematic Chain Developed to Characterize Walking with Sensor Deployment

$$T_i^{i-1} = \begin{bmatrix} \cos\theta_i & -\sin\theta_i\cos\alpha_i & \sin\theta_i\sin\alpha_i & a_i\cos\theta_i \\ \sin\theta_i & \cos\theta_i\cos\alpha_i & -\cos\theta_i\sin\alpha_i & a_i\sin\theta_i \\ 0 & \sin\alpha_i & \cos\alpha_i & d_i \\ 0 & 0 & 0 & 1 \end{bmatrix}, \tag{1}$$

Table 1: D-H Parameters in the Tracking Protocol of Walking

i	d_i	θ_i	**i**	d_i	θ_i	**i**	d_i	θ_i
1	d_1	$\pi/2$	4	0	θ_4	7	0	θ_7
2	d_2	$\pi/2$	5	0	θ_5	8	0	θ_8
w	d_3	$\pi/2$	t	L_{ht}	θ_6	l	L_{kl}	θ_9
3	d_3	$\pi/2$	6	L_{hk}	θ_6			

where a_i is the distance from O_i to the intersection of the x_i and z_{i-1} axes along x_i; d_i is the distance from O_{i-1} to the intersection of the x_i and z_{i-1} axes along z_{i-1}; α_i is the angle between z_{i-1} and z_i measured about x_i; and θ_i is the angle between x_{i-1} and x_i measured about z_{i-1} [7]. If the joint between Link $i-1$ and Link i is prismatic, d_i will be variable. Otherwise, it will be θ_i. Table 1 shows the D-H parameters in the tracking protocol of walking where L_{ht} is the distance from hip to the sensor mounting position on the thigh, L_{hk} is the distance from hip to knee, L_{kl} is the distance from knee to the sensor mounting position on leg (a_i and α_i are always 0 and $\pi/2$ in our case).

2.2. Velocity and Acceleration Propagation

Sensors are applied at the waist, thigh and leg (Fig. 1) with their measurements yielding information related to segment movements from the base (Link 0) up to the point of sensor application. This section discusses the propagation of velocity and acceleration from link to link.

In walking, body segments experience two kinds of movements: translation and rotation. Thus, we need to derive both linear and angular velocity and acceleration of the sensor mounted body segments. The angular velocity of Link $i+1$ is the angular velocity propagated from Link i plus the new component added by Joint $i+1$

$$\omega_{i+1}^i = R_{i-1}^i \omega_i^{i-1} + \dot{\theta}_{i+1} z_i^i, \tag{2}$$

where R_{i-1}^i is the transpose of the top-left 3×3 sub-matrix of T_i^{i-1}. The linear velocity of Link $i+1$ is the linear velocity propagated from Link i plus the component caused by the rotational velocity of Link i plus the new component added by Joint $i+1$

$$v_{i+1}^i = R_{i-1}^i (v_i^{i-1} + \omega_i^{i-1} \times O_i^{i-1}) + \dot{d}_{i+1} z_i^i, \tag{3}$$

where O_i^{i-1} is the top-right 3×1 vector of T_i^{i-1}. By calculating the derivative, the angular and linear acceleration from Link i to Link $i+1$ is formulated in Eq. (4) and (5).

$$\dot{\omega}_{i+1}^i = \dot{\theta}_i z_{i-1}^{i-1} \times R_{i-1}^i \omega_i^{i-1} + R_{i-1}^i \dot{\omega}_i^{i-1} + \ddot{\theta}_{i+1} z_i^i, \tag{4}$$

$$\begin{aligned} \dot{v}_{i+1}^i &= \dot{\theta}_i z_{i-1}^{i-1} \times R_{i-1}^i (v_i^{i-1} + \omega_i^{i-1} \times O_i^{i-1}) + R_{i-1}^i \dot{v}_{i+1}^i \\ &+ R_{i-1}^i (\dot{\omega}_i^{i-1} \times O_i^{i-1}) + R_{i-1}^i (\omega_i^{i-1} \times \dot{d}_i z_{i-1}^{i-1}) + \ddot{d}_{i+1} z_i^i. \end{aligned} \tag{5}$$

2.3. Tracking Algorithm

9DOF sensors integrated with a 3-axis accelerometer, a 3-axis gyroscope and a 3-axis magnetometer are used to collect motion data. In this section, we formulate the state model and measurement model to estimate the joint configuration from the sensor signals.

The state transition equations, which describe the evolution of joint configuration are given by

$$\ddot{d}_i[n+1] = \alpha_l \ddot{d}_i[n] + u_l[n] \tag{6}$$

$$\theta_j[n+1] = \theta_j[n] + \dot{\theta}_j[n]T + \frac{1}{2}\ddot{\theta}_j[n]T^2 \tag{7}$$

$$\dot{\theta}_j[n+1] = \dot{\theta}_j[n] + \ddot{\theta}_j[n]T \tag{8}$$

$$\ddot{\theta}_j[n+1] = \alpha_a \ddot{\theta}_j[n] + u_a[n], \tag{9}$$

where $i = \{1, 2, 3\}$ and $j = \{4, ..., 9\}$, $\ddot{d}_i[n]$ is the linear acceleration of Joint i at time n, $\theta_j[n]$, $\dot{\theta}_j[n]$, and $\ddot{\theta}_j[n]$ is the angular displacement, velocity and acceleration of Joint j at time n, $u_l[n]$ and $u_a[n]$ are both white noise processes with zero mean, α_l and α_a are process model parameters, and T is the sampling period. These formulations were derived following the assumption that both the linear and angular accelerations are constant during a sampling interval and they can be fit into a first-order zero-mean autoregressive process characterized by parameter α_l and α_a.

The measurement equations, which describe the relationship between the joint configuration and sensor measurements are given by

$$z_a^w[n] = R_0^w g^0 + R_2^w \dot{v}_w^2[n] + v_a^w[n], \tag{10}$$

$$z_a^t[n] = R_0^t g^0 + R_5^t \dot{v}_t^5[n] + v_a^t[n], \tag{11}$$

$$z_g^t[n] = R_5^t \omega_t^5[n] + v_g^t[n], \tag{12}$$

$$z_m^t[n] = R_0^t m^0 + v_m^t[n], \tag{13}$$

$$z_a^c[n] = R_0^c g^0 + R_8^c \dot{v}_c^8[n] + v_a^c[n], \tag{14}$$

$$z_g^c[n] = R_8^c \omega_c^8[n] + v_g^c[n], \tag{15}$$

$$z_m^c[n] = R_0^c m^0 + v_m^c[n], \tag{16}$$

where $z_a^w[n]$ is the measurement of the waist accelerometer at time n, $z_a^t[n]$, $z_g^t[n]$, and $z_m^t[n]$ is the measurement of the thigh accelerometer, gyroscope and magnetometer at time n, $z_a^c[n]$, $z_g^c[n]$, and $z_m^c[n]$ is the measurement from the leg sensor at time n, $v_a^w[n]$, $v_a^t[n]$, $v_g^t[n]$, $v_m^t[n]$, $v_a^c[n]$, $v_g^c[n]$, and $v_m^c[n]$ are all white noise processes with zero mean, and g^0 and m^0 is the gravity and magnetic field projected in Link 0. The propagation of kinematic parameters between two arbitrary links such as $\dot{v}_w^2[n]$ can be formulated based on the recursive equations introduced in Section 2.2.

Filtering technique is used to track the dynamic joint configuration by two steps, state update and measurement update. We assume within a gait cycle, linear displacement of the body center is dominated by the component along the walking direction and the thigh and leg rotation is on the Sagittal Plane.

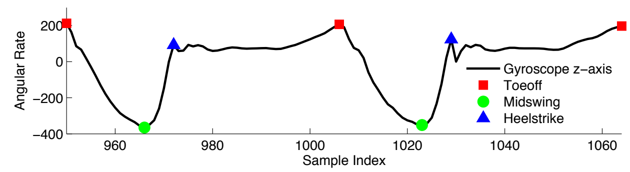

Fig. 2: Detection of Walking Phases in a Gait Cycle.

These constraints are incorporated into an Unscented Kalman filter by projecting the sigma points which are outside the feasible region onto the boundary of the feasible region in the time-update step [10]. Another assumption to model walking is based on the observation that when one leg is in mid-swing, the other will be in mid-stance with the hip, knee and ankle joint in a line perpendicular to the ground. Thus, a 3-axis gyroscope is placed on the opposite leg to detect the mid-swing, which corresponds to the mid-stance of the tracked leg. This information can be used to reset the state vector periodically by the same projection method. In addition, a backward filter is applied within each gait cycle where the mid-stance signifies the start and the end. Overall, a constrained forward-backward statistical linearized sigma-point Kalman Smoother [11, 12] is used with periodic state vector resetting to track walking.

3. EXPERIMENT

3.1. Data Collection

Four 9DOF Razor IMUs are used to acquire motion data and the measurements are sent wirelessly through a bluetooth modem to a tablet. Sensors were attached to subjects' waist, thigh and leg with the x-y plane aligned with the Sagittal Plane and the y-axis along the gravity. All the sensors were sampling at $50Hz$ and signature motions were put at the start and end of each data sequence for synchronization. Stride length was measured directly using a ruled floor surface as well as a means of marking shoe contact by application of marking liquid to the shoe.

3.2. Walking Phase Detection

The walking phases of interest are toe-off, mid-stance and heel-strike, where toe-off and heel-strike are used to estimate step length (described in the subsequent section). Previous work introduced walking phase decomposition using a foot-mounted gyroscope [13]. Since our sensor deployment is different, the signals of an ankle and foot mounted gyroscope are compared. Fig. 2 shows the decomposition result using an ankle-mounted gyroscope.

3.3. Visual Reconstruction and Step Length Estimation

The tracking algorithm yields the dynamic joint configuration which is used to render visual reconstruction of body motions. However, since the accelerometer is the only sensor to collect body translation related measurements, this estimate is not sufficiently trustworthy. Thus, only thigh and leg rotation were reconstructed. From the visual reconstruction, the algorithm of walking phase detection is verifiable.
Step length can be estimated through motion reconstruction. The component of the linear displacement of foot from toe-off to heel-strike along the axis of walking direction was calculated as L. Since L only accounts for the displacement caused by segment rotation, a linear model was applied to estimate the step length in order to compensate the component of body translation, which is formulated as

$$SL = a \times L + b, \tag{17}$$

where SL is the step length, and a and b are two parameters that need to be trained.

3.4. Result

The tracking algorithm has been tested on 10 subjects, whose hip positions vary from 1.09m to 1.44m measuring from the ground. Every subject walked normally for approximately 40 strides in each trial after a short pause to initialize the tracking algorithm (sample $z_a^t[0]$, $z_m^t[0]$. $z_a^c[0]$, $z_m^c[0]$ and the gyroscope offset). Fig. 3 illustrates an example of the estimation result of the six revolute joint configuration during walking by employing different algorithms (only the last few steps were cropped for better illustration). Comparison were made among the regular Unscented Kalman filter (UKF), the constrained UKF assuming limb rotation is exclusively on the Sagittal Plane, the constrained UKF with periodic state vector resetting and the constrained forward-backward statistical linearized sigma-point Kalman Smoother with periodic state vector resetting. By noting that walking is a repetitive activity, the plot indicates that the regular UKF and the constrained UKF will drift after long time tracking, especially the constrained UKF, which is quite sensitive to defective sensor measurements (seen between Sample Index 2100 and 2150) while the constrained UKF with periodic state vector resetting and the constrained forward-backward statistical linearized sigma-point Kalman Smoother with periodic state vector resetting perform much more stably since their estimates between two different gait cycles are relatively independent. The difference between the results of these two methods are negligible.

Outputs were collected from the constrained forward-backward statistical linearized sigma-point Kalman Smoother with periodic state vector resetting and input into a rigid body to render 3D reconstruction of thigh and leg rotation (Fig. 4), from where L was calculated.

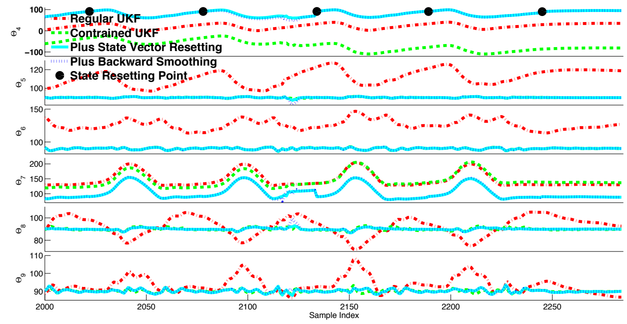

Fig. 3: Estimation of Joint Configuration During Walking.

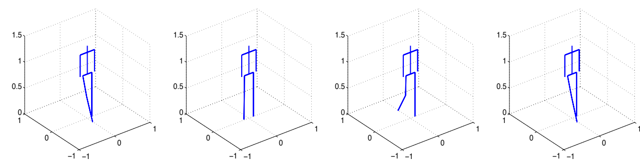

(a) Heelstrike (b) Midstance (c) Toeoff (d) Heelstrike

Fig. 4: Motion Reconstruction of Key Walking Phases.

Fig. 5: Step Length Estimation Error.

Three different models were used to train and test the step length estimation algorithm, intra-subject model (each subject has a separate set of parameters), inter-subject model (all the subjects share the same parameters) and intra-cluster model where subjects were assigned into a set of groups based on their step length using K-Means Clustering method and a and b were trained within individual clusters. The cross-validation method was adopted to evaluate the system performance. Fig. 5 shows the step length estimation error by using 30% of the data for training and 70% for testing and both the intra-subject model and intra-clustered model (with more than 3 clusters) give almost 96% accuracy. Note that on average, each subject has 30 steps with both sensor measurements and step length ground truth.

4. CONCLUSION

This paper introduced and demonstrated the new concept of activity-specific motion tracking protocols and introduced a trunk-thigh-leg kinematic chain to model walking that can be directly extended to track other activities. The designed tracking algorithm shows very stable performance for extended time period tracking and achieves nearly 96% accuracy for step length estimation exceeding the performance of prior work [9].

5. REFERENCES

[1] B. Dobkin and A. Dorsch, “The promise of mhealth daily activity monitoring and outcome assessments by wearable sensors,” *Neurorehabilitation and Neural Repair*, vol. 25, no. 9, pp. 788–798, 2011.

[2] N. Gordon, M. Gulanick, F. Costa, G. Fletcher, B. Franklin, E. Roth, and T. Shephard, “Physical activity and exercise recommendations for stroke survivors an american heart association scientific statement from the council on clinical cardiology, subcommittee on exercise, cardiac rehabilitation, and prevention; the council on cardiovascular nursing; the council on nutrition, physical activity, and metabolism; and the stroke council,” *Circulation*, vol. 109, no. 16, pp. 2031–2041, 2004.

[3] P.-C. Chung, Y.-L. Hsu, C.-Y. Wang, C.-W. Lin, J.-S. Wang, and M.-C. Pai, “Gait analysis for patients with alzheimer’s disease using a triaxial accelerometer,” in *Circuits and Systems (ISCAS), 2012 IEEE International Symposium on*, may 2012, pp. 1323 –1326.

[4] L. Yan, L. Yue-e, and H. Jian, “Gait recognition based on mems accelerometer,” in *Signal Processing (ICSP), 2010 IEEE 10th International Conference on*, oct. 2010, pp. 1679 –1681.

[5] J. Hamill and K. Knutzen, *Biomechanical Basis of Human Movement with Motion Analysis Software*. Lippincott Williams & Wilkins, 2006.

[6] D. M. Morris, G. Uswatte, J. E. Crago, E. W. Cook, and E. Taub, “The reliability of the wolf motor function test for assessing upper extremity function after stroke,” *Archives of Physical Medicine and Rehabilitation*, vol. 82, pp. 750 – 755, 2001.

[7] M. Spong and M. Vidyasagar, *Robot dynamics and control*. John Wiley & Sons, 2008.

[8] M. El-Gohary, L. Holmstrom, J. Huisinga, E. King, J. McNames, and F. Horak, “Upper limb joint angle tracking with inertial sensors,” in *Engineering in Medicine and Biology Society,EMBC, 2011 Annual International Conference of the IEEE*, 30 2011-sept. 3 2011, pp. 5629 –5632.

[9] K. Nagarajan, N. Gans, and R. Jafari, “Modeling human gait using a kalman filter to measure walking distance,” in *Proceedings of the 2nd Conference on Wireless Health*, ser. WH ’11. New York, NY, USA: ACM, 2011, pp. 34:1–34:2.

[10] R. Kandepu, L. Imsland, and B. Foss, “Constrained state estimation using the unscented kalman filter,” in *Control and Automation, 2008 16th Mediterranean Conference on*, june 2008, pp. 1453 –1458.

[11] A. Paul and E. Wan, “A new formulation for nonlinear forward-backward smoothing,” in *Acoustics, Speech and Signal Processing, 2008. ICASSP 2008. IEEE International Conference on*, 31 2008-april 4 2008, pp. 3621 –3624.

[12] M. Gao, Z. He, and Y. Liu, “Improved unscented kalman filter for bounded state estimation,” in *Electronics, Communications and Control (ICECC), 2011 International Conference on*, sept. 2011, pp. 2101 –2104.

[13] A. Sabatini, C. Martelloni, S. Scapellato, and F. Cavallo, “Assessment of walking features from foot inertial sensing,” *Biomedical Engineering, IEEE Transactions on*, vol. 52, no. 3, pp. 486 –494, march 2005.